Inorg. Chem. **2005**, *44*, 7606–7615

The Synthesis, Structural, and Spectroscopic Characterization of Uranium(IV) Perrhenate Complexes

Gordon H. John,[†] Iain May,*[,†] Clint A. Sharrad,[†] Andrew D. Sutton,[†] David Collison,[‡] Madeleine Helliwell,[‡] and Mark J. Sarsfield[§]

Centre for Radiochemistry Research, School of Chemistry, The University of Manchester, Oxford Road, Manchester, M13 9PL United Kingdom, and Nexia Solutions, Sellafield, Seascale, Cumbria, CA20 1PG United Kingdom

Received May 18, 2005

We report the synthesis, structural, and spectroscopic characterization of a series of uranium(IV)–perrhenato complexes. Three isostructural complexes with general formula $[U(ReO_4)_4(L)_4]$ (where L = tri-*n*-butylphosphine oxide/TBPO (**2**), triethyl phosphate/TEP (**3**), or tri-*iso*-butyl phosphate/T^{i}BP (**4**)), have been synthesized, both through the photoreduction of ethanolic $\{UO_2\}^{2+}$ solutions and also via a novel U^{IV} starting material, $U(ReO_4)_4 \cdot 5H_2O$ (**1**). Compound **1** has also been used in the preparation of $[U(ReO_4)_4(TPPO)_3(CH_3CN)] \cdot 2CH_3CN$ (**5**) and $[U(ReO_4)(DPPMO_2)_3(OH)][ReO_4]_2 \cdot 2CH_3CN$ (**6**), where TPPO represents triphenylphosphine oxide and $DPPMO_2$ represents bis(diphenylphosphino)methane dioxide. All six complexes have been spectroscopically characterized using NMR, UV–vis–NIR, and IR techniques, with **2**, **3**, **5**, and **6** also fully structurally characterized. The U atoms in compounds **2-6** all exhibit eight-coordinate geometry with up to four perrhenate groups in addition to three ($DPPMO_2$ and TPPO) or four (TEP, T^{i}BP, TBPO) coordinated organic ligands. In the case of compounds **5** and **6**, the coordination of eight ligands to the U^{IV} center is completed by the binding of a solvent molecule (CH_3CN) and OH^-, respectively. Solid-state physical analysis (elemental and thermogravimetric) and infrared spectroscopy are in agreement with the structural studies. The crystallographic data suggest that the strength of the U^{IV}–O-donor ligand bonds decreases across the series $R_3PO > [ReO_4]^- > (RO)_3PO$. Solution-state IR and ^{31}P NMR spectroscopy appear to be in agreement with these solid-state results.

Introduction

In recent years, we have started to investigate the interaction between the pertechnetate anion, $[TcO_4]^-$, and actinide cations with the aim of gaining insight into $[TcO_4]^-$ behavior during nuclear fuel processing and nuclear waste treatment.[1] We have previously reported the structural characterization of $[UO_2(TcO_4)_2(TPPO)_3]$ [2] (TPPO = triphenylphosphine oxide) and solution-phase stability of $[UO_2(TcO_4)(DPPMO_2)_2]^+$ ($DPPMO_2$ = bis(diphenylphosphino)methane dioxide),[3] while other researchers have structurally characterized $[(NpO_2)_2(TcO_4)_2(H_2O)_3]$.[4] In each case, the pertechnetate anion directly coordinates to the actinide metal center. We were interested in extending this chemistry to U^{IV}, particularly due to the observation that $[TcO_4]^-$ can oxidize U^{IV} to the uranyl dication, $\{UO_2\}^{2+}$.[5] However, this redox activity greatly prohibits the direct study of U^{IV}–$[TcO_4]^-$ coordination chemistry, although by switching to redox inactive (under these conditions) Th^{IV} we have been able to prepare the pertechnetate complex $[Th(TcO_4)_4(TBPO)_4]$.[2] In addition, investigations into the U^{IV}–$[ReO_4]^-$ system should be feasible because the $[ReO_4]^-$ anion is much less oxidizing

* To whom correspondence should be addressed. E-mail: Iain.May@man.ac.uk.
[†] Centre for Radiochemistry Research, School of Chemistry, The University of Manchester.
[‡] School of Chemistry, The University of Manchester.
[§] Nexia Solutions.

(1) *The Nuclear Fuel Cycle*; Wilson, P. D., Ed.; Oxford University Press: Oxford, 1986.
(2) Sarsfield, M. J.; Sutton, A. D.; May, I.; John, G. H., Sharrad, C.; Helliwell, M. *Chem. Commun*. **2004**, 2320.
(3) Sutton, A. D.; John, G. H.; Sarsfield, M. J.; Renshaw, J. C.; May, I.; Martin, L. R.; Selvage, A. J.; Collison, D.; Helliwell, M. *Inorg. Chem*. **2004**, *43*, 5480.
(4) Fedosseev, A. M.; Budantseva, N. A.; Grigoriev, M. S.; Guerman, K. E. *Radiochemistry* **2003**, *91*, 147.
(5) (a) Kemp, T. J.; Thyer, A. M.; Wilson, P. D. *J. Chem. Soc., Dalton Trans*. **1993**, 2601. (b) Kemp, T. J.; Thyer, A. M.; Wilson, P. D. *J. Chem. Soc., Dalton Trans*. **1993**, 2607. (c) Garraway, J.; Wilson, P. D. *J. Less-Common Met*. **1984**, *97*, 191.

10.1021/ic0507971 CCC: $30.25 © 2005 American Chemical Society
Published on Web 09/13/2005

than $[TcO_4]^-$. This would allow the $U^{IV}-[TcO_4]^-$ system to be studied indirectly through both U (Th) and Tc (Re) analogues. The coordination chemistry of $[ReO_4]^-$ with a range of transition metals has previously been studied,[6] and we have shown that perrhenate is an excellent analogue of pertechnetate in our systems with the structural characterization of perrhenate analogues of $[UO_2(TcO_4)_2(TPPO)_3]$[7] and $[UO_2(TcO_4)(DPPMO_2)_2]^+$.[3]

In this paper, we report the first structural characterization of a series of uranium(IV) perrhenate complexes, in all four cases in the presence of P═O donor ligands (phosphate or phosphine oxide). P═O donor ligands have been employed in the synthesis of our previous uranyl and thorium $[TcO_4]^-/[ReO_4]^-$ complexes,[2−3,7] many U^{IV} complexes with P═O ligands have already been structurally characterized,[8] and most solvent extraction operations in the nuclear industry are performed with tri-*n*-butyl phosphate.[1] Two synthetic routes were employed: photoreduction of $\{UO_2\}^{2+}$ in EtOH in the presence of $[ReO_4]^-$ and direct synthesis through a novel starting reagent, $U(ReO_4)_4{\cdot}5H_2O$.

Experimental Section

Caution. *Both natural and depleted uranium were used during the course of these experiments. As well as the radioactive hazards associated with ^{238}U and ^{235}U, uranium is a toxic metal, and care should be taken with all manipulations.*

General. All chemicals were reagent grade, obtained commercially and used as supplied except for UO_3 and UCl_4 which were obtained from the Centre for Radiochemistry Research isotope stocks. Apart from the photolytic methods of preparation of $[U(ReO_4)_4(L_4)]$ (where L = TBPO (**2**), TEP (**3**), and T^iBP (**4**)), all preparative work was carried out under an inert atmosphere (Ar or N_2) using standard Schlenk and dried, degassed solvent techniques. IR spectra were recorded on a Bruker Equinox 55/Bruker FRA 106/5 with a coherent 500 mW laser. Solid and solution samples were recorded as attenuated total reflectance (ATR) spectra using a "Golden Gate" attachment. ^{31}P solution-state NMR spectra were performed using a Bruker Avance Ultrashield 400 MHz spectrometer using appropriate deuterated solvent as a lock with 5 mm diameter NMR tubes. Electronic absorption spectroscopy measurements were recorded using a Cary Varian 500 Scan UV−vis−NIR spectrophotometer, typically over the scan range 200−900 nm (solvent dependent) at a scan rate of 600 nm min^{-1}. Thermogravimetric analysis was carried out under N_2 using a Mettler Toledo TGA/SDTA 851^e analyzer on samples heated in alumina crucibles over the temperature range 25−900 °C at a rate of 5 °C min^{-1} (see Supporting Information). Elemental analysis was carried out using a Carlo Erba Instruments CHNS-O EA1108 elemental analyzer (C, H, and N analysis) and a Fisons Horizon Elemental Analysis ICP-OES spectrometer (metal analysis).

Syntheses. $U(ReO_4)_4{\cdot}5H_2O$ (1). UCl_4 (1.12 g, 2.96 mmol) was dissolved in $HReO_4$ (3.06 g, 12.0 mmol) to form an immediate dark green precipitate that was filtered and dried in vacuo to yield a dark green solid (3.69 g, 99% yield), which was stored under N_2. Anal. Calcd for $H_{10}O_{21}Re_4U$: H, 0.76; Re, 56.07; U, 17.92. Found: H, 0.70; Re, 56.73; U, 17.73%. The presence of five water molecules was confirmed by thermogravimetric analysis (see Supporting Information).

$[U(ReO_4)_4(TBPO)_4]$ (2). Method 1. A yellow solution of $[UO_2(ReO_4)_2{\cdot}H_2O]$[9] (0.25 mmol, 200 mg) and TBPO (0.50 mmol, 0.110 g) in EtOH (4 mL) was allowed to evaporate slowly in direct sunlight. The solution turned dark green after 1 week, and green prismatic crystals formed 2 weeks later. The solution was decanted off and a sticky crystalline solid collected (0.060 mg, 22% yield). Anal. Calcd for $C_{48}H_{108}O_{20}P_4Re_4U$: C, 27.29; H, 5.16; P, 5.87; Re, 35.27; U, 11.27. Found: C, 26.89; H, 4.85; P, 5.67; Re, 34.97; U, 11.88%.

Method 2. $U(ReO_4)_4{\cdot}5H_2O$ (93 mg, 0.075 mmol) was dissolved in acetonitrile (1.0 mL) to give a dark green solution. TBPO (654 mg, 0.300 mmol) in acetonitrile (1.0 mL) was then added. The resulting solution was stored under N_2 overnight to yield dark green block crystals (146 mg, 92% yield). Anal. Calcd for $C_{48}H_{108}O_{20}P_4Re_4U$: C, 27.29; H, 5.16; P, 5.87; Re, 35.27; U, 11.27. Found: C, 27.19; H, 5.41; P, 6.12; Re, 34.85; U, 11.59%.

$[U(ReO_4)_4(TEP)_4]$ (3). Method 1. A solution of TEP (1.40 mmol, 0.164 mL) in toluene (3 mL) was added dropwise to UO_3 (0.70 mmol, 200 mg) dissolved in $HReO_4$ (1.40 mmol, 0.192 mL). The toluene was removed in vacuo to leave a viscous yellow oil. After 10 weeks in direct sunlight, green block crystals were removed from the oil, carefully washed with toluene, and dried (0.205 mg, 30% yield). Anal. Calcd for $C_{24}H_{60}O_{32}P_4Re_4U$: C, 14.63; H, 3.08; P, 6.29; Re, 37.81; U, 12.08. Found: C, 14.40; H, 2.84; P, 6.37; Re, 37.03; U, 12.46%.

Method 2. $U(ReO_4)_4{\cdot}5H_2O$ (186 mg, 0.150 mmol) was dissolved in acetonitrile (1.0 mL) and TEP (109 mg, 0.600 mmol) added. Crystals were grown overnight at room temperature (255 mg, 87% yield). Anal. Calcd for $C_{24}H_{60}O_{32}P_4Re_4U$: C, 14.63; H, 3.08; P, 6.29; Re, 37.81; U, 12.08. Found: C, 14.83; H, 3.00; P, 6.64; Re, 38.33; U, 12.31%.

$[U(ReO_4)_4(T^iBP)_4]$ (4). Method 1. A yellow solution of $[UO_2(ReO_4)_2{\cdot}H_2O]$ (0.25 mmol, 200 mg) and T^iBP (0.50 mmol, 0.135 cm^3) in EtOH (4 mL) was allowed to evaporate slowly in direct sunlight. The solution turned dark green after 1 week, and green block crystals formed 4 weeks later. The solution was decanted off and a oil covered crystalline solid collected (0.102 mg, 35% yield). Anal. Calcd for $C_{48}H_{108}O_{32}P_4Re_4U$: C, 25.02; H, 4.73; P, 5.38; Re, 32.32; U, 10.33. Found: C, 24.22; H, 4.34; P, 5.71; Re, 31.97; U, 10.99 %.

Method 2. $U(ReO_4)_4{\cdot}5H_2O$ (186 mg, 0.150 mmol) was dissolved in acetonitrile (1.0 mL) and T^iBP (160 mg, 0.060 mmol) added. Crystals were grown overnight at room temperature from the resultant solution (300 mg, 87% yield). Anal. Calcd for $C_{48}H_{108}O_{32}P_4Re_4U$: C, 25.02; H, 4.73; P, 5.38; Re, 32.32; U, 10.33. Found: C, 25.08; H, 4.81; P, 5.57; Re, 31.51; U, 10.00%.

$[U(ReO_4)_4(TPPO)_3(CH_3CN)]{\cdot}2CH_3CN$ (5). $U(ReO_4)_4{\cdot}5H_2O$ (186 mg, 0.150 mmol) was dissolved in acetonitrile (1.0 mL) to give a dark green solution. TPPO (167 mg, 0.600 mmol) in acetonitrile (1.0 mL) was then added. The resulting solution was stored under N_2 overnight to yield dark green block crystals (258 mg, 84% yield). Anal. Calcd for $C_{60}H_{54}N_3O_{19}P_3Re_4U$: C, 32.73;

(6) See, for example: Chakrovarti, M. C. *Coord. Chem. Rev.* **1990**, *106*, 205.
(7) John, G. H.; May, I.; Sarsfield, M. J.; Steele, M. H.; Collison, D.; Helliwell, M.; McKinney, J. D. *Dalton Trans.* **2004**, 734.
(8) See, for example: (a) du Preez, J. G. H.; Gellatly, B. J.; Jackson, G.; Nassimbeni, L. R.; Rodgers, A. L. *Inorg. Chim. Acta* **1978**, *27*, 181. (b) Avens, L. A.; Barnhart, D. M.; Burns, C. J.; McKee, S. D. *Inorg. Chem.* **1996**, *35*, 537. (c) Day, J. P.; Venazi, L. M. *J. Chem. Soc. A* **1966**, 197. (d) Dillen, J. L.; can Rooyen, P. H.; Strydom, C. A.; van Vuuren, C. P. J. *Acta Crystallogr., Sect. C* **1988**, *44*, 1921. (e) Charpin, P. P.; Lance, M.; Soulie, E.; Vigner, D.; Marquet-Ellis, H. *Acta Crystallogr., Sect. C* **1985**, *41*, 1723.
(9) Zaitseva, L. L.; Velichko, A. V.; Kolomeitsev, G. Yu. *Russ. J. Inorg. Chem.* **1982**, *27*, 1625.

Table 1. Crystallographic Data for $[U(ReO_4)_4(TBPO_4)]$ (**2**), $[U(ReO_4)_4(TEP)_4]$ (**3**), $[U(ReO_4)_4(TPPO)_3(CH_3CN)]\cdot 2CH_3CN$ (**5**), and $[U(ReO_4)(DPPMO_2)_3(OH)][ReO_4]_2\cdot 2CH_3CN$ (**6**)

	2	**3**	**5**	**6**
empirical formula	$C_{48}H_{108}O_{20}P_4Re_4U$	$C_{24}H_{56}O_{32}P_4Re_4U$	$C_{60}H_{54}N_3O_{19}P_3Re_4U$	$C_{79}H_{73}N_2O_{19}P_6Re_3U$
fw	2112.05	1963.40	2196.80	2336.84
space group	*Cc*	$P42_1c$	$P2_1/c$	$P2_1/c$
cryst group	monoclinic	tetragonal	monoclinic	monoclinic
a (Å)	21.40(2)	13.4198(13)	18.3426(13)	13.2883(7)
b (Å)	21.68(2)	13.4198(13)	18.5254(13)	29.7796(16)
c (Å)	14.78(2)	14.932(2)	19.2253(14)	20.2358(11)
α (deg)	90	90	90	90
β (deg)	90.00(3)	90	95.0640(10)	90.1710(10)
γ (deg)	90	90	90	90
V (Å^3)	6857(13)	2689.1(15)	6507.3(8)	8007.7(7)
Z	4	2	4	4
T (K)	100(2)	150(2)	293(2)	293(2)
λ (Å)	0.71069	0.71069	0.71073	0.71073
abs coeff (mm^{-1})	9.545	12.174	10.040	6.727
R1, wR2 indices ($I > 2\sigma^2$)	0.0322, 0.0799	0.0240, 0.0521	0.0501, 0.1231	0.0432, 0.0918
R indices (all data)	0.0329, 0.0803	0.0268, 0.0528	0.0660, 0.1356	0.0617, 0.1114

H, 2.70; N, 1.91; P, 4.22; Re, 33.83; U, 10.83. Found: C, 32.50; H, 2.20; N, 1.54; P, 4.22; Re, 32.27; U, 10.99%.

$[U(ReO_4)(DPPMO_2)_3(OH)][ReO_4]_2\cdot 2CH_3CN$ (6). $U(ReO_4)_4\cdot 5H_2O$ (186 mg, 0.150 mmol) was dissolved in acetonitrile (1.0 mL) to give a dark green solution. $DPPMO_2$ (189 mg, 0.450 mmol) in acetonitrile (1.0 mL) was then added. The solution was stored at 4 °C for several days to form dark green rod-shaped crystals (197 mg, 63% yield). Anal. Calcd for $C_{79}H_{73}N_2O_{19}P_6Re_3U$: C, 40.48; H, 3.42; N, 1.20; P, 7.93; Re, 23.84; U, 10.16. Found: C, 40.85; H, 3.63; N, 1.20; P, 7.99; Re, 23.93; U, 10.06%.

Single-Crystal X-ray Diffraction. The crystallographic data for $[U(ReO_4)_4(TBPO)_4]$ (**2**), $[U(ReO_4)_4(TEP)_4]$ (**3**), $[U(ReO_4)_4(TPPO)_3(CH_3CN)]\cdot 2CH_3CN$ (**5**), and $[U(ReO_4)(DPPMO_2)_3(OH)][ReO_4]_2\cdot 2CH_3CN$ (**6**) are summarized in Table 1. Diffraction data for **2** were collected on a Rigaku RAXIS diffractometer at 100 K. Diffraction data for **3**, **5**, and **6** were measured on a Bruker APEX SMART platform CCD at 100 K. Structures were solved by direct methods using SIR97,[10] SHELXL97[11] (**2**, **5** and **6**), and SHELXTL[12] (**3**). The cell parameters were refined by full-matrix least squares. All non-hydrogen atoms were refined anisotropically, while hydrogen atoms were included in calculated positions. Restraints were used on the anisotropic thermal motion of all C-atoms. Compound **2** could be solved in three different, temperature-dependent, space groups, and a more detailed analysis of the data collection and structure refinement will be presented elsewhere.[13]

Results and Discussion

Synthesis and Physical Characterization. The syntheses of $[U(ReO_4)_4(TBPO)_4]$ (**2**), $[U(ReO_4)_4(TEP)_4]$ (**3**), and $[U(ReO_4)_4(T^iBP)_4]$ (**4**), where TBPO, TEP, and T^iBP are tri-*n*-butylphosphine oxide, triethyl phosphate, and tri-*iso*-butyl phosphate, respectively, were initially undertaken serendipitously. Our attempts to synthesize additional P═O donor ligand complexes analogous to $[UO_2(ReO_4)_2(TPPO)_3]$ in ethanolic solution resulted in a color change from yellow to green, with the concomitant growth of absorption bands characteristic of U^{IV} (λ_{max} = 429, 486, 495, 549, 646, and 672 nm),[14] followed by the precipitation of crystalline products of either **2**, **3**, or **4**. With hindsight, this is not unexpected, and the photolytic reduction of the uranyl ion to the tetravalent state, especially in alcohols, is well documented.[15] We have also prepared all three complexes directly from a novel U^{IV} starting material, $[U(ReO_4)_4]\cdot 5H_2O$ (**1**), as confirmed by vibrational spectroscopy. This reagent has also been used to prepare $[U(ReO_4)_4(TPPO)_3(CH_3CN)]\cdot 2CH_3CN$ (**5**) and $[U(ReO_4)(DPPMO_2)_3(OH)][ReO_4]_2\cdot 2CH_3CN$ (**6**). As well as characterization by elemental analysis, all six compounds were characterized by TGA (see Supporting Information).

Single-Crystal X-ray Diffraction. The structure of $[U(ReO_4)_4(TBPO)_4]$ (**2**) (Figure 1) shows a monomeric uranium(IV) complex containing four TBPO and four monodentate perrhenate ligands isostructural with $[Th(TcO_4)_4(TBPO)_4]$.[2] The eight-coordinate uranium atom is at

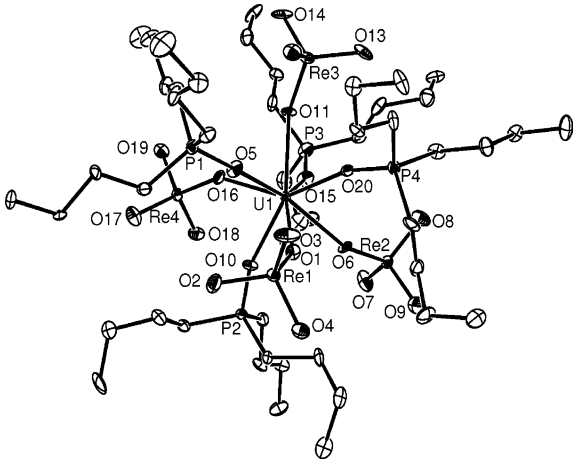

Figure 1. ORTEP plot of the structure of $[U(ReO_4)_4(TBPO)_4]$ (**2**). Probability ellipsoids of 30% are shown.

(10) *SIR97*: Altomare, A.; Burla, M. C.; Camalli, M.; Cascarano, G. L.; Giacovazzo, C.; Guagliardi, A.; Moliterni, A. G. G.; Polidri, G.; Spagna, R. *J. Appl. Crystallogr*. **1999**, *32*, 115.
(11) *SHELXL97*: Sheldrick, G. M. *Programme for crystal structure refinement*; The University of Göttingen: Göttingen, Germany,1997.
(12) *SHELXTL*: *SHELX-PC Package*; Bruker Analytical X-ray Systems: Madison, WI, 1998.
(13) Helliwell, M.; Collison, D.; John, G. H.; May, I.; Sarsfield, M. J.; Sharrad, C. A.; Sutton, A. D. *Acta Crystallogr,. Sect. B*, in press.
(14) Katz, J. J.; Seaborg, G. T.; Morss, L. R. *The Chemistry of the Actinide Elements*, 2nd ed.; Chapman and Hall Ltd.: London, 1986.
(15) (a) Burrows, H. D.; Kemp, T. J. *Chem. Soc. Rev*. **1974**, *3*, 139. (b) Adamson, A. W.; Waltz, W. L.; Zinato, E.; Watts, D. W.; Fleischauer, P. D.; Lindholm, R. D. *Chem. Rev*. **1972**, *68*, 541. (c) Ohyoshi, A.; Ueno, K. *J. Inorg. Nucl. Chem*. **1974**, *36*, 379. (d) Matsushima, R.; Sakuraba, S. *J. Am. Chem. Soc*. **1971**, *93*, 5421.

Table 2. Selected Bond Lengths [Å] and Angles [deg] for $[U(ReO_4)_4(TBPO)_4]$ (**2**)

U(1)−O(1)	2.436(7)	U(1)−O(11)	2.442(10)
U(1)−O(5)	2.282(7)	U(1)−O(15)	2.306(8)
U(1)−O(6)	2.425(7)	U(1)−O(16)	2.421(10)
U(1)−O(10)	2.306(11)	U(1)−O(20)	2.313(11)
O(5)−U(1)−O(15)	137.0(3)	O(10)−U(1)−O(11)	148.9(4)
O(10)−U(1)−O(15)	95.6(4)	O(15)−U(1)−O(11)	72.7(3)
O(5)−U(1)−O(20)	91.1(4)	O(20)−U(1)−O(11)	71.4(4)
O(10)−U(1)−O(20)	139.6(3)	O(16)−U(1)−O(11)	76.6(3)
O(15)−U(1)−O(20)	103.2(4)	O(6)−U(1)−O(11)	123.5(3)
O(5)−U(1)−O(16)	73.7(3)	O(1)−U(1)−O(11)	131.3(4)
O(10)−U(1)−O(16)	72.5(4)	O(5)−U(1)−O(1)	74.6(3)
O(15)−U(1)−O(16)	72.7(3)	O(10)−U(1)−O(1)	72.4(4)
O(20)−U(1)−O(16)	147.3(4)	O(15)−U(1)−O(1)	148.3(3)
O(5)−U(1)−O(6)	152.8(3)	O(20)−U(1)−O(1)	73.0(4)
O(10)−U(1)−O(6)	75.8(4)	O(16)−U(1)−O(1)	127.3(4)
O(15)−U(1)−O(6)	70.1(3)	O(6)−U(1)−O(1)	78.5(3)
O(20)−U(1)−O(6)	77.5(4)	O(5)−U(1)−O(11)	74.0(3)
O(16)−U(1)−O(6)	127.6(4)	O(5)−U(1)−O(10)	99.2(4)

the center of a dodecahedron,[16] with selected bond lengths and angles listed in Table 2.

The $U-O_{(TBPO)}$ bond distances in $[U(ReO_4)_4(TBPO)_4]$ (**2**) are the same within error (2.282(7)−2.313(11) Å), and only the shortest bond is significantly different from all of the comparative $U-O_{(P=O)}$ bonds in $[U(NCS)_4(TPPO)_4]$ [17] and in $[U(NCS)_4(TMPO)_4]$[18] (where TMPO = trimethylphosphine oxide) (averages 2.35 and 2.32 Å, respectively). Comparisons of $U^{IV}-O_{(perrhenate)}$ and $U^{VI}-O_{(perrhenate)}$ bond distances are, to an extent, possible because of the similarities in effective nuclear charge, Z_{eff}, of U^{VI} (+3.3) and U^{IV} (+4).[14] With this in mind, the $U^{IV}-O_{(perrhenate)}$ bond distances are the same within error (2.421(10)−2.442(10) Å) and comparable to the average $U^{VI}-O_{(perrhenate)}$ bond length in $[UO_2(ReO_4)_2(TPPO)_3]$ (2.403(4) Å).[9]

The U−O−P (154.7(5)−166.1(6)°) and U−O−Re bond angles (147.4(5)−154.3(4)°) cover a wide range, as previously also observed in $[UO_2(ReO_4)_2(TPPO)_3]$ (139.2(2)−162.7(3)°, 137.5(2)°, and 150.7(2)°, respectively).[9] The most distorted perrhenate group contains O−Re−O bond angles between 106.1(7)° and 112.5(6)°. Distortions in the geometry of dodecahedral complexes are not uncommon,[19] but combined with the slight deformation of the perrhenate groups and the size of the TBPO ligands, this may suggest that some of the distortion in $[U(ReO_4)_4(TBPO)_4]$ (**2**) is caused by steric effects. The distortion may also be explained by considering the solid-state packing. Molecules pack in a zigzag arrangement within the lattice, with the uranium atom enclosed by TBPO and $[ReO_4]^-$ groups. Intramolecular interactions between H-atoms of the TBPO groups and O-atoms of the $[ReO_4]^-$ in the molecule (closest separation = 2.673(19) Å) may affect the geometries of these functional groups.

The asymmetric unit of $[U(ReO_4)_4(TEP)_4]$ (**3**) contains a quarter of the molecule consisting of a $UReO_8PC_6H_{15}$ unit where a 4-fold symmetry operation on the site of the U atom yields the entire complex. The structure (Figure 2) shows a monomeric uranium(IV) complex of similar geometry to $[U(ReO_4)_4(TBPO)_4]$ (**2**), containing four TEP and four monodentate perrhenate ligands. The eight-coordinate uranium atom is at the center of a dodecahedron,[16] with selected bond lengths and angles listed in Table 3.

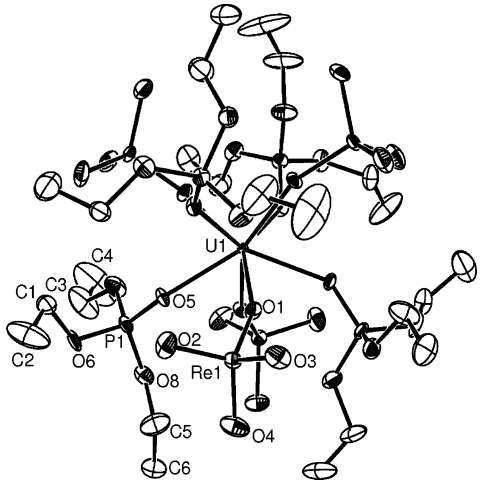

Figure 2. ORTEP plot of the structure of $[U(ReO_4)_4(TEP)_4]$ (**3**). Probability ellipsoids of 30% are shown.

Table 3. Selected Bond Lengths [Å] and Angles [deg] for $[U(ReO_4)_4(TEP)_4]$ (**3**)

U(1)−O(1)	2.293(4)	U(1)−O(5)	2.392(4)
O(1)−U(1)−O(1^{I})[a]	142.3(2)	O(5)−U(1)−O(1^{II})	71.80(15)
O(1)−U(1)−O(1^{II})	95.99(7)	O(5)−U(1)−O(1^{III})	145.89(15)
O(5)−U(1)−O(1)	73.81(14)	O(5)−U(1)−O(5^{I})	74.1(2)
O(5)−U(1)−O(1^{I})	76.30(13)	O(5)−U(1)−O(5^{II})	129.54(13)

[a] I, II, and III are 4-fold symmetry generated oxygen atoms.

The $U^{IV}-O_{(TEP)}$ bond distance of 2.392(4) Å is similar to the average $U^{IV}-O_{(TPPO)}$ bond length in $[U(NCS)_4(TPPO)_4]$[17] (2.35 Å) but is longer than the average $U^{IV}-O_{(TBPO)}$ distance in $[U(ReO_4)_4(TBPO)_4]$ (**2**; 2.302 Å) and shorter than $U^{VI}-O_{(TEP)}$ distances in $[UO_2(NO_3)_2(TEP)_2]$[20] (2.44 Å). The $U^{IV}-O_{(perrhenate)}$ bond distance is 2.293(4) Å, which is significantly shorter than the comparable bond lengths in **2** (2.421(10)−2.442(10) Å) and the average $U^{VI}-O_{(perrhenate)}$ distances in $[UO_2(ReO_4)_2(TPPO)_3]$ (2.403(4) Å). Direct comparison of all the U−O bond lengths in **2** and **3** $[U(ReO_4)_4(TEP)_4]$ (**3**) suggests that the strength of O-donor ligand interaction with U^{IV} follows the order TBPO > $[ReO_4]^-$ > TEP, although it would be inappropriate to rely solely on observed bond lengths to compare U−O bond strengths.

The U−O−P angle in $[U(ReO_4)_4(TEP)_4]$ (**3**) is very acute (141.2(3)°) compared with the U−O−P angles in $[U(ReO_4)_4(TBPO)_4]$ (**2**; 154.7(5)−166.1(6)°), while the U−O−Re angle is very obtuse (157.1(2)°) compared to those in **2** (147.4(5)−154.3(4)°). The perrhenate groups have regular geometries with $Re-O_{(terminal)}$ bond lengths of 1.693(4), 1.709(4), and 1.709(5) Å and O−Re−O bond angles between 109.2(2)° and 109.8(2)°. As might be expected, a longer Re−O bond length (1.766(4) Å) is observed for the O-atom also coordinated to uranium. Molecules pack in a cubic arrange-

(16) Determined by the criteria set out in the following: Haigh, C. W. *Polyhedron* **1995**, *14*, 2871.
(17) Bombieri, G.; De Paoli, G.; Forsellini, E. *J. Inorg. Nucl. Chem.* **1979**, *32*, 2181.
(18) Rickard, C. E. F.; Woollard, D. C. *Aust. J. Chem.* **1979**, *32*, 2181.
(19) Kepert, D. L.; Patrick, J. M.; White, A. H. *J. Chem. Soc., Dalton Trans.* **1983**, 385.
(20) Fleming, J. E.; Lynton, H. *Chem. Ind.* **1960**, 1415.

ment, the uranium atom enclosed by TEP and $[ReO_4]^-$ groups. Intramolecular and intermolecular interactions between H-atoms of the TEP ligands and O-atoms of the perrhenate groups (closest separations = 2.766(5) and 2.746(5) Å, respectively) do not appear to result in a distortion of the dodecahedral geometry, unlike the situation found in **2**. This would suggest that the more bulky TBPO ligands in **2** may be the cause of these distortions.

The connectivity has also been established for $[U(ReO_4)_4(T^iBP)_4]$ (**4**) using a low-resolution X-ray diffraction study. A disordered molecular structure shows a monomeric uranium(IV) complex, containing four T^iBP and four monodentate perrhenate ligands. The molecule probably has a similar geometry to that of $[U(ReO_4)_4(L)_4]$ (where L = TBPO (**2**) and TEP (**3**)), with the eight-coordinate uranium atom at the center of a dodecahedron.

There are many examples of eight-coordinate U^{IV} structures listed in the current version of the Cambridge Structural Database,[21] although only seven of these have the general formula $[U(X)_4(Y)_4]$ (where X and Y are monodentate ligands), as observed for $[U(ReO_4)_4(L)_4]$ (where L = TBPO (**2**), TEP (**3**), and T^iBP (**4**)). Of these seven structures, four are of the general type $[U(NCS)_4(Y)_4]$ (where Y = Me_3PO, Ph_3PO, $(NMe_2)_3PO$, and H_2O)[17−19,22] and have square antiprismatic geometries. The compounds $[U(NCS)_4(MeCON\{^iPr\}_2)_4]$,[23] $[UCl_4(MeCN)_4]$,[24,25] and $[UCl_4(^iPrOH)_4]$[26] are all assigned dodecahedral coordination geometries, each with varying degrees of distortion.

The structure of $[U(ReO_4)_4(TPPO)_3(CH_3CN)]\cdot 2CH_3CN$ (**5**) shows a monomeric uranium(IV) complex with four coordinated perrhenates, three coordinated TPPO ligands, and a coordinated acetonitrile molecule (Figure 3). The eight-coordinate U^{IV} compound has a dodecahedral geometry,[16] and there are four molecules in the unit cell. In the crystal structure, one perrhenate is disordered over two sites, 4A and 4B. From analysis of the thermal factors, this perrhenate is in the 4A position at 66.6% occupancy and 4B position at 33.3% occupancy. The structure of **5** differs from those of $[U(ReO_4)_4(L)_4]$ (where L = TBPO (**2**), TEP (**3**), and T^iBP (**4**)) through the replacement of one P=O donor ligand by a coordinated solvent molecule. This is almost certainly due to the increased steric bulk of TPPO versus TBPO, T^iBP, or TEP. Selected bond lengths and angles are shown in Table 4.

All three $U-O_{(TPPO)}$ bond lengths are the same, within error (U(1)−O(3), 2.286(8); U(1)−O(2), 2.294(9); U(1)−O(1), 2.315(9) Å). The $U-O_{(TPPO)}$ bond lengths are comparable to previously structurally characterized U^{IV}−TPPO complexes (for $[U(OTf)_4(TPPO)_3]$[27] the $U-O_{(TPPO)}$ bond lengths are 2.207(3), 2.252(3), and 2.318(3) Å, while for $[U(BH_4)_4(TPPO)_2]$[28] they are 2.33(2) and 2.24(2) Å). The U−O−P bond angles show variation (167.4(5)°, 171.4(6)°, and 160.8(5)°), with the ligand in closest proximity to the perrhenates being most obtuse. In $[U(BH_4)_4(TPPO)_2]$, the two U−O−P angles are also different with angles of 156(1)° and 168(1)°.[28]

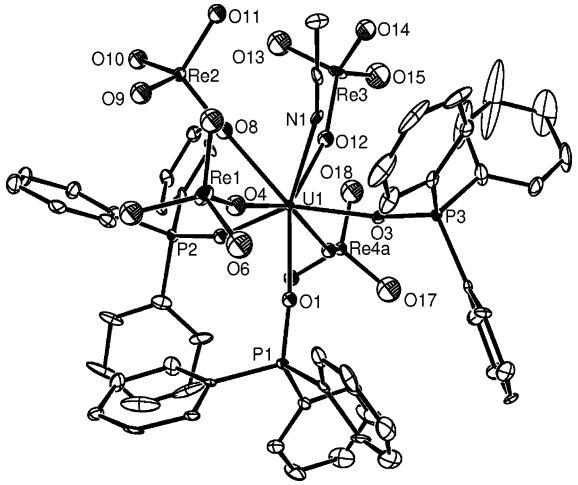

Figure 3. ORTEP plot of the structure of $[U(ReO_4)_4(TPPO)_3(CH_3CN)]\cdot 2CH_3CN$ (**5**). Probability ellipsoids of 30% are shown.

Table 4. Selected Bond Lengths [Å] and Angles [deg] for $[U(ReO_4)_4(TPPO)_3(CH_3CN)]\cdot 2CH_3CN$ (**5**)

U(1)−O(3)	2.286(8)	U(1)−O(12)	2.339(9)
U(1)−O(2)	2.294(9)	U(1)−O(16)	2.349(8)
U(1)−O(4)	2.313(9)	U(1)−O(8)	2.398(9)
U(1)−O(1)	2.315(9)	U(1)−N(1)	2.586(12)
O(3)−U(1)−O(2)	148.5(3)	O(12)−U(1)−O(16)	71.6(3)
O(3)−U(1)−O(4)	104.6(3)	O(3)−U(1)−O(8)	137.9(3)
O(2)−U(1)−O(4)	94.1(3)	O(2)−U(1)−O(8)	71.5(3)
O(3)−U(1)−O(1)	77.6(3)	O(4)−U(1)−O(8)	73.4(3)
O(2)−U(1)−O(1)	84.0(3)	O(1)−U(1)−O(8)	136.6(3)
O(4)−U(1)−O(1)	73.2(3)	O(12)−U(1)−O(8)	72.1(3)
O(3)−U(1)−O(12)	84.3(3)	O(16)−U(1)−O(8)	123.9(3)
O(2)−U(1)−O(12)	99.7(3)	O(12)−U(1)−N(1)	73.6(3)
O(4)−U(1)−O(12)	136.2(3)	O(16)−U(1)−N(1)	134.6(3)
O(1)−U(1)−O(12)	149.2(3)	O(8)−U(1)−N(1)	69.3(3)
O(3)−U(1)−O(16)	77.6(3)	O(3)−U(1)−N(1)	70.9(3)
O(2)−U(1)−O(16)	74.2(3)	O(2)−U(1)−N(1)	140.4(3)
O(4)−U(1)−O(16)	152.0(3)	O(4)−U(1)−N(1)	69.5(3)
O(1)−U(1)−O(16)	80.2(3)	O(1)−U(1)−N(1)	122.0(3)

The shortest $U-O_{(perrhenate)}$ bond length in $[U(ReO_4)_4(TPPO)_3(CH_3CN)]\cdot 2CH_3CN$ (**5**; 2.313(9) Å) is significantly shorter than the $U-O_{(perrhenate)}$ bond lengths in $[U(ReO_4)_4(TPBO)_4]$ (**2**; average 2.431(9) Å) whereas the longest $U-O_{(perrhenate)}$ bond length in **5** (2.398(9) Å) is significantly longer than the $U-O_{(perrhenate)}$ bond length in $[U(ReO_4)_4(TEP)_4]$ (**3**; 2.203(4) Å). The $U^{IV}-O_{(perrhenate)}$ bond lengths are also shorter than the $U^{VI}-O_{(perrhenate)}$ bond lengths of $[UO_2(ReO_4)_2(TPPO)_3]$[7] (average = 2.403(4) Å) which might be, at least partly, due to the increase of effective nuclear

(21) Allen, F. H.; Davies, J. E.; Galloy, J. J.; Johnson, O.; Kennard, O.; Macrae, C. F.; Mitchell, E. M.; Mitchell, G. F.; Smith, J. M.; Watson, D. G. *J. Chem. Inf. Comput. Sci.* **1991**, *31*, 187.
(22) Charpin, P.; Costes, R. M.; Folcher, G.; Plurien, P.; Navaza, A.; de Rango, C. *Inorg. Nucl. Chem. Lett.* **1977**, *13*. 341.
(23) Al-Daher, A. G. M.; Bagnall, K. W.; Castellani, C. B.; Benetollo, F.; Bombieri, G. *Inorg. Chim. Acta* **1984**, *95*, 269.
(24) Cotton, F. A.; Marler, D. O.; Schwotzer, W. *Acta Crystallogr., Sect. C* **1984**, *40*, 1186.
(25) den Bossche, G. V.; Rebizant, J.; Spirlet, M. R.; Goffart, J. *Acta Crystallogr,. Sect. C* **1986**, *42*, 1478.
(26) Gordon, P. L.; Thompson, J. A.; Watkin, J. G.; Burns, C. J.; Sauer, N. N.; Scott, B. L. *Acta Crystallogr., Sect. C* **1999**, *55*, 1275.
(27) Berthet, J. C.; Nierlich, M.; Ephritikhine, M. *Eur. J. Inorg. Chem.* **2002**, *4*, 850.
(28) Charpin, P. P.; Nierlich, M.; Chevrier, G.; Vigner, D.; Lance, M.; Baudry, D. *Acta Crystallogr., Sect. C.* **1987**, *43*, 1255.

charge, Z_{eff}, associated with U^{IV} (+4.0) versus U^{VI} (+3.3).[14] The coordinating Re−O bond lengths are all the same within error (1.744(9)−1.775(8) Å) and tend to be longer than the noncoordinating Re−O bond lengths, although these do show more variation (1.618(12)−1.742(13) Å). This is indicative of a degree of distortion in the bound perrhenates. The bond angles confirm this distortion with O−Re−O angles ranging between 102.4(7)° and 122.0(3)° for Re(1) and Re(4A), respectively. Re(4B) exhibits an even larger degree of distortion with O−Re−O angles between 92.5(10)° and 129.9(6)°.

The U−N bond length for the coordinated acetonitrile (2.586(12) Å) is comparable to that in $[UCl_4(CH_3CN)_4]$,[24] where crystallographically inequivalent U−N bond lengths are 2.577(14) and 2.601(13) Å, respectively. The internal N≡C−C acetonitrile bond angle is 179.0(15)°, and the N−C bond length is 1.139(17) Å, again comparable to that in $[UCl_4(CH_3CN)_4]$ (178.0(2)° and 179.0(2)° and 1.12(2) and 1.15(2) Å, respectively).[24]

With regard to the molecular packing, the four coordinated $[ReO_4]^-$ anions form a hydrophilic core. Adjacent molecules are packed in a "head-to-tail" arrangement in alternating rows. This leads to the coordinated $[ReO_4]^-$ anions being totally encapsulated in a hydrophobic shell of coordinated TPPOs from adjacent molecules (see Supporting Information).

The fact that only three TPPO ligands coordinated in $[U(ReO_4)_4(TPPO)_3(CH_3CN)]\cdot 2CH_3CN$ (**5**) (vs 4 P═O donor ligands in $[U(ReO_4)_4(L_4)]$ where L = TBPO (**2**), TEP (**3**), and T^iBP (**4**)) is not surprising and is probably due to steric constraints. No uranium complex has yet been crystallographically characterized with more than three coordinated TPPO ligands, which is highlighted by the formation of the analogous complex $[U(OTf)_4(TPPO)_3]$.[27] This was crystallized in the presence of excess TPPO with weakly coordinating triflate, and eight-coordination is achieved by triflate exhibiting rare bidentate coordination rather than U^{IV} coordinating to a fourth TPPO group.

The crystal structure of $[U(ReO_4)(DPPMO_2)_3(OH)][ReO_4]_2\cdot 2CH_3CN$ (**6**) shows a monomeric uranium(IV) complex with one coordinated perrhenate, three coordinated bidentate $DPPMO_2$ ligands, and a coordinated hydroxide resulting in a dicationic species with the charge balanced by two uncoordinated perrhenate counteranions (Figure 4). This is the first reported example of a U^{IV}−$DPPMO_2$ complex and an actinide complex with three coordinated bidentate $DPPMO_2$ ligands. The eight-coordinate U^{IV} molecule possesses dodecahedral geometry[16] with four molecules in the unit cell. Selected bond lengths and angles are given in Table 6.

Apart from one significantly longer bond length (2.482(6) Å) and more obtuse chelate bite angle (74.0(2)°), the bond lengths and angles for the three coordinated $DPPMO_2$ ligands in **6** are comparable to those observed in the other uranium−$DPPMO_2$ complexes.[3,29−30] Two of the ligands

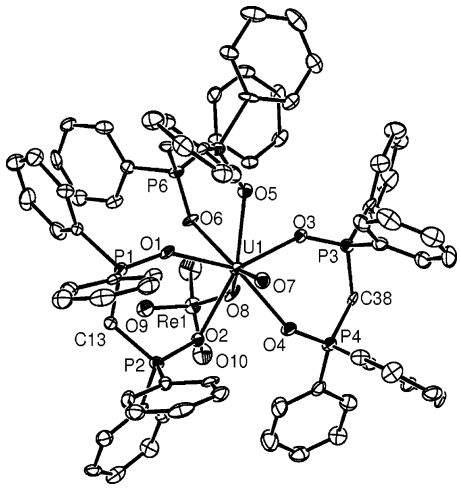

Figure 4. ORTEP plot of the structure of $[U(ReO_4)(DPPMO_2)_3(OH)][ReO_4]_2\cdot 2CH_3CN$ (**6**). Probability ellipsoids of 30% are shown.

Table 5. Selected Bond Lengths [Å] and Angles [deg] for $[U(ReO_4)(DPPMO_2)_3(OH)][ReO_4]_2\cdot 2CH_3CN$ (**6**)

U(1)−O(7)	2.137(7)	U(1)−O(4)	2.405(6)
U(1)−O(5)	2.379(6)	U(1)−O(8)	2.411(7)
U(1)−O(3)	2.394(7)	U(1)−O(1)	2.438(7)
U(1)−O(2)	2.394(6)	U(1)−O(6)	2.482(6)
O(7)−U(1)−O(5)	79.6(2)	O(4)−U(1)−O(8)	71.3(2)
O(7)−U(1)−O(3)	97.9(2)	O(7)−U(1)−O(1)	82.8(2)
O(5)−U(1)−O(3)	69.7(2)	O(5)−U(1)−O(1)	75.8(2)
O(7)−U(1)−O(2)	90.2(2)	O(3)−U(1)−O(1)	144.8(2)
O(5)−U(1)−O(2)	149.1(2)	O(2)−U(1)−O(1)	74.0(2)
O(3)−U(1)−O(2)	140.9(2)	O(4)−U(1)−O(1)	140.3(2)
O(7)−U(1)−O(4)	77.1(2)	O(8)−U(1)−O(1)	118.5(2)
O(5)−U(1)−O(4)	131.9(2)	O(7)−U(1)−O(6)	145.0(2)
O(3)−U(1)−O(4)	72.6(2)	O(5)−U(1)−O(6)	71.9(2)
O(2)−U(1)−O(4)	72.2(2)	O(3)−U(1)−O(6)	91.0(2)
O(7)−U(1)−O(8)	147.9(2)	O(2)−U(1)−O(6)	104.0(2)
O(5)−U(1)−O(8)	126.8(2)	O(4)−U(1)−O(6)	137.5(2)
O(3)−U(1)−O(8)	78.4(2)	O(8)−U(1)−O(6)	67.1(2)
O(2)−U(1)−O(8)	74.9(2)	O(1)−U(1)−O(6)	71.1(2)

contain long and short $U-O_{(P=O)}$ bonds as previously observed in some of the reported actinide complexes that have been structurally characterized and also in the transition metal complexes $[Ni(DPPMO_2)_3][ClO_4]_2\cdot MeOH$[31] and $[Fe(DPPMO_2)_3][I_3]$.[32]

The $U-O_{(perrhenate)}$ bond length is longer (2.411(7) Å) than that in $[U(ReO_4)_4(TPPO)_3(CH_3CN)]\cdot 2CH_3CN$ (**5**; average = 2.350(9) Å), $[U(ReO_4)_4(TEP)_4]$ (**3**; average = 2.293(4) Å), and $[UO_2(ReO_4)(DPPMO_2)_2][ReO_4]$ (2.336(6) Å),[3] although it is comparable to that in $[U(ReO_4)_4(TEP)_4]$ (**2**; average = 2.431(9) Å). The coordinating Re−O bond (1.747(7) Å) is comparable to the coordinating Re−O bond length in **5** (1.744(9)−1.775(8) Å), **2** (1.736(7)−1.768(11) Å), and **3** (1.766(4) Å). The noncoordinated Re−O bond lengths vary slightly (1.696(7), 1.696(7), and 1.721(8) Å), and the O−Re−O bond angles range from 107.8(4)° to 111.8(4)°, indicating less distortion from tetrahedral geometry than coordinated perrhenates in **5** (102.4(7)° and 122.0(3)°). Interestingly, the two uncoordinated $[ReO_4]^-$ anions also

(29) Kannan, S.; Rajalakshmi, N.; Chetty, K. V.; Venugopal, V.; Drew, M. G. B. *Polyhedron* **2004**, *23*, 1527.
(30) John, G. H.; May, I.; Collison, D.; Helliwell, M. *Polyhedron* **2004**, *23*, 3097.
(31) Bermejo, E.; Castineiras, A.; Dominguez, R.; Schule, C. *J. Coord. Chem.* **1994**, *33*, 353.
(32) Barclay, J. E.; Evans, D. J.; Hughes, D. L.; Leigh, G. L. *J. Chem. Soc., Dalton Trans.* **1993**, 69.

have similar Re−O bond lengths (1.676(9) and 1.747(8) Å) and O−Re−O bond angles (105.81(47)° and 111.80(49)°) compared to those of the coordinated $[ReO_4]^-$. The $U-O_{(OH)}$ bond length is 2.137(7) Å, comparable to the $U-O_{(O-H)}$ bond lengths in the U^{IV} complex $[U(tpa)_2(OH)_2]I_2 \cdot 3CH_3CN$ (tpa = tris[(2-pyridyl)methyl]amine) (2.1269(12) and 2.1465(13) Å).[33]

Two $[U(ReO_4)(DPPMO_2)_3(OH)]^{2+}$ molecules of **6** pack as two hemispheres with the perrhenates pointing into the center yielding a hydrophilic core (see Supporting Information). The central perrhenates line up along one axis in a staggered conformation with the closest intramolecular distance between noncoordinating oxygens of adjacent perrhenates (3.245(11) Å). This results in a hydrophilic core surrounded by a hydrophobic shell as can be seen clearly in the space filling diagram. The noncoordinated $[ReO_4]^-$ species sit outside the hydrophobic shell, but they are partially surrounded by adjacent cation pairs.

In **6**, three $DPPMO_2$ ligands and only one $[ReO_4]^-$ and one OH^- anion are coordinated in the dication $[U(ReO_4)(DPPMO_2)_3(OH)]^{2+}$ with two additional $[ReO_4]^-$ counteranions. In d-transition metals, it has previously been shown that $DPPMO_2$ can stabilize cationic complexes,[31−32] and this has also been seen in the uranyl perrhenate complex $[UO_2(ReO_4)(DPPMO_2)_2]^+$.[3] Clearly, the stability of chelating bidentate $DPPMO_2$ compares favorably with the ability of coordinated $[ReO_4]^-$ to neutralize the U^{IV} positive charge. Interestingly, the presence of coordinated OH^-, presumably through deprotonation of water present in CH_3CN, indicates that $DPPMO_2$ is not that effective at U^{IV} charge neutralization. The presence of U^{IV}-bound OH^- instead of a second $[ReO_4]^-$ anion probably also reflects the steric constraints placed on the complex by the presence of three bulky $DPPMO_2$ groups. However, it should be noted that in the presence of more strongly coordinating counteranions (F^- and NO_3^-) charge-neutral complexes are observed ($[UO_2(\mu\text{-}F)(F)(DPPMO_2)]_2$[30] and $[UO_2(NO_3)_2(DPPMO_2)]$,[29] respectively).

Infrared Spectroscopy. The solid- and solution-state infrared spectra were collected for $[U(ReO_4)_4(L_4)]$ (where L = TBPO (**2**), TEP (**3**), and T^iBP (**4**)), $[U(ReO_4)_4(TPPO)_3(CH_3CN)] \cdot 2CH_3CN$ (**5**), and $[U(ReO_4)(DPPMO_2)_3(OH)][ReO_4]_2$ (**6**), with only the solid-state measurement for $U(ReO_4)_4 \cdot 5H_2O$. All the spectra are provided as Supporting Information, along with peak assignments. Raman spectra on the deep green compounds could not be obtained due to the absorption of the laser, and subsequent sample decomposition, even at low power (50 mW).

Solid State. The most diagnostic stretch within the organic ligand is the $\nu_{(P=O)}$, and as expected, there are observable lower energy shifts of this band upon complexation to the U^{IV} metal resulting from the reduction in P═O bond strength. $[U(ReO_4)_4(L_4)]$ (where L = TBPO (**2**), TEP (**3**), and T^iBP (**4**)) and $[U(ReO_4)_4(TPPO)_3(CH_3CN)] \cdot 2CH_3CN$ (**5**) all give a single vibration for the P═O stretch indicating a single, monodentate binding mode (for example, $\nu_{(P=O)}$ for TPPO shifts from 1186 to 1047 cm^{-1} on coordination in **2**). However, the $DPPMO_2$ complex (**6**) gives at least two overlapping bands, possibly a reflection of the different chemical environments of the P═O ligand in the crystal structure. For $[U(ReO_4)_4(TPPO)_3(CH_3CN)] \cdot 2CH_3CN$, weak peaks for coordinated and free acetonitrile are observed at 2268 and 2243 cm^{-1}, respectively.[34] Coordinated hydroxide for $[U(ReO_4)(DPPMO_2)_3(OH)][ReO_4]_2$ can be seen in the spectra at 1587, 2931, and 3053 cm^{-1}.[34]

Free perrhenate, which retains its tetrahedral geometry, gives two infrared active fundamentals, ν_3 (916 cm^{-1}) and ν_4 (332 cm^{-1}). For monodentate coordination, the ν_3 and ν_4 should split into two bands, and the ν_1 and ν_2 vibrations should be observed in the infrared spectra. In the case of bidentate or bridging coordination modes, three bands should be observed for ν_3 and ν_4 in addition to the single bands for ν_1 and ν_2.[6]

Perrhenate vibrations in the infrared have been studied extensively for d-transition metal complexes[6] and inorganic uranyl perrhenate complexes including $[UO_2(ReO_4)_2(H_2O)]$,[35] $[UO_2(OH)(ReO_4)(H_2O)]$, and $[UO_2(OH)(ReO_4)]$.[9] In addition, we have previously assigned bands for $[ReO_4]^-$ coordinated to $\{UO_2\}^{2+}$.[9] On the basis of this work, $\nu_1-\nu_4$ bands have been assigned for all the synthesized compounds indicating coordinated $[ReO_4]^-$ in all six cases. The assignment of at least four ν_3 and two ν_4 bands in $U(ReO_4)_4 \cdot 5H_2O$ (**1**) indicates the presence of bridging $[ReO_4]^-$. In $[U(ReO_4)_4(L_4)]$ (where L = TEP (**3**) and T^iBP (**4**)) and $[U(ReO_4)(DPPMO_2)_3(OH)][ReO_4]_2 \cdot 2CH_3CN$ (**6**), ν_3 is split into three bands, rather than the expected two for monodentate coordination. For **6** this can be attributed to the additional presence of noncoordinated $[ReO_4]^-$. In compounds **3** and **4**, the reason is less obvious, with monodentate coordination only observed crystallographically. Tentatively, therefore, the additional bands may be ascribed to lattice packing effects in the crystal.

Solution State. Samples for solution infrared measurements were prepared by dissolving approximately 5−20 mg of sample in a solvent in which the complex was most soluble. Unfortunately, in all cases, the solvent can coordinate to U^{IV} (i.e., CH_3CN, pyridine, or MeOH), potentially displacing coordinated P═O donor ligand or $[ReO_4]^-$. Measurements on the solution were carried out, and the free solvent spectrum was subtracted.

The solution spectrum for $[U(ReO_4)_4(TPPO)_3(CH_3CN)] \cdot 2CH_3CN$ (**5**) dissolved in CH_3CN gives strong peaks at 1038, 918, and 831 cm^{-1}. These peaks can be assigned as coordinated TPPO vibrations and two ν_3 (Re═O) vibrations, respectively. The other strong bands can be assigned to TPPO ligand vibrations. The P═O vibration is shifted slightly with respect to the solid spectrum (1047 cm^{-1}) but is still indicative of coordination. In the free ligand, the P═O peak occurs at 1186 cm^{-1}, and a very weak vibration is observed

(33) Karmazin, L.; Mazzanti, M.; Pécaut, J. *Inorg. Chem.* **2003**, *42*, 5900.

(34) Nakamoto, K. *Infrared and Raman Spectra of Inorganic and Coordination Compounds; Parts A and B*, 5th ed.; John Wiley and Sons Ltd.: New York, 1997.

(35) John, G. H. PhD Thesis, The University of Manchester, 2003.

at this wavenumber in the solution spectrum indicating some noncoordinated TPPO. The presence of two strong ν_3 $[ReO_4]^-$ vibrations and a low intensity peak at 986 cm^{-1}, which can be tentatively assigned to ν_1, indicates that $[ReO_4]^-$ is still coordinated. However, the ν_3 bands come at different wavenumbers in solution with respect to the solid state. This may either be attributed to different speciation in the solid state versus solution or to the absence of lattice effects in solution.

The solution spectrum for $[U(ReO_4)_4(TBPO)_4]$ (**2**) dissolved in CH_3CN is relatively poorly resolved although a shoulder is observed at 1053 cm^{-1} assigned to the P═O vibration of TBPO coordinated to U^{IV}. A strong vibration at 1036 cm^{-1} is also related to the coordinated ligand. This is in comparison to the solid state where the P═O vibration is observed at 1057 cm^{-1} as a shoulder on a band at 1032 cm^{-1}. Additional vibrations at 847 and 831 cm^{-1} are also likely to correspond to the ligand. No peaks assignable to $[ReO_4]^-$ vibrations were observed.

The spectrum for $[U(ReO_4)(DPPMO_2)_3(OH)](ReO_4)_2 \cdot 2CH_3CN$ (**6**) carried out in pyridine shows similarities to the solid-state spectra with a vibrational band observed at 1065 cm^{-1} assigned to coordinated P═O. In the solid state, the P═O vibration was assigned to a pair of peaks at 1064 and 1074 cm^{-1}, but presumably in solution the ligands are less constrained resulting in a single equivalent vibration. A strong peak is present at 908 cm^{-1} with a shoulder at 932 cm^{-1} for the ν_3 vibration. The presence of the 908 cm^{-1} peak at much higher intensity in relation to the second peak at 932 cm^{-1} may be suggesting the presence of a large percentage of uncoordinated perrhenate in solution, especially as no band attributable to the ν_1 $[ReO_4]^-$ vibration was observed. For pyridine, there are no vibrational bands between 760 and 970 cm^{-1}. However, there are three strong bands for pyridine at 989, 1030, and 1067 cm^{-1}, which may account for weak additional bands in the observed solution spectra.

For $[U(ReO_4)_4(T^iBP)_4]$ (**4**) dissolved in MeOH, peaks associated with coordinated T^iBP are largely absent in comparison to the solid state. The spectrum has more bands in common with uncoordinated T^iBP, with peaks shared with the free ligand at 1252, 1099, 1072, and 1000 cm^{-1}. Most interesting is the apparent splitting of the $[ReO_4]^-$ ν_3 vibration into at least four bands at 943, 924, 908, and 885 cm^{-1} (see Figure 5). The splitting pattern is distinctly different from that observed in the solid state. This suggests that the perrhenate is acting either as a bridging or bidentate ligand in order to help fill the coordination sphere of the U^{IV} in the absence of coordinated T^iBP. Alternatively, this could suggest the presence of more than one species in solution. In addition, the band at 964 cm^{-1} could be assigned to the ν_1 symmetric stretch of coordinated $[ReO_4]^-$.

The solution spectrum of $[U(ReO_4)_4(TEP)_4]$ (**3**) dissolved in MeOH gives a weak peak at 1165 cm^{-1} for coordinated P═O and additional peaks corresponding to coordinated TEP (1098, 1174, and 1049 cm^{-1}). This indicates a stronger TEP interaction with U^{IV} in relation to T^iBP although there are peaks in the spectra related to the free ligand at 1165, 1097,

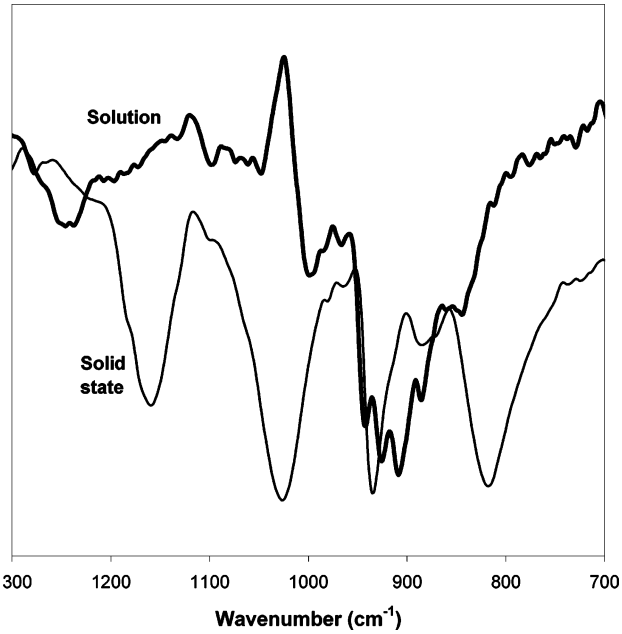

Figure 5. Mid-infrared ATR (in transmission) of $[U(ReO_4)_4(T^iBP)_4]$ (**4**) dissolved in MeOH (bold) and in solid state (thin).

1074, and 1000 cm^{-1}. As for the T^iBP complex (**4**), the perrhenate ν_3 peak is again split into three distinctive, strong peaks at 941, 925, and 907 cm^{-1} with a shoulder at 887 cm^{-1} indicating a bidentate or bridging bonding mode or the presence of more than one species in solution.

The solution infrared spectra have shown there is a definite difference between the solid- and solution-state speciation. For the TBPO (**2**) and TPPO (**5**) complexes, it is apparent that the affinity of U^{IV} for the P═O donor ligands is higher than for perrhenate in solution. In $[U(ReO_4)(DPPMO_2)_3(OH)](ReO_4)_2 \cdot 2CH_3CN$ (**6**), there is possibly still a degree of interaction between U^{IV} and perrhenate although this cannot be confirmed due to the presence of perrhenate acting as a counteranion in this compound and the dominance of the unbound perrhenate peaks. For complexes with TEP and T^iBP, either there is definitely a mixture of species with coordinated monodentate perrhenate in solution or the perrhenate is acting as a bidentate or bridging ligand resulting in the further splitting of the ν_3 vibration. There is also clear evidence for uncoordinated TEP and T^iBP present on dissolution of complexes **3** and **4**, respectively. Therefore, it would appear that **2**−**5** are unstable with respect to ligand exchange in coordinating solvents. In addition, the strength of ligand interaction in U^{IV} appears to follow the order phosphine oxide > perrhenate > phosphate.

NMR Spectroscopy. Variable temperature (218−298 K) ^{31}P NMR spectra were recorded in various solvents, depending on complex solubility for **2**−**6**. At room temperature, a characteristic shift of the ^{31}P NMR signal due to coordination of the P═O donor ligands is observed for all complexes. For example, on coordination of TPPO to U^{IV} in **5** the peak is shifted downfield from 32.49 to 46.67 ppm. For **2**−**5**, a single peak is observed indicative of a single phosphorus environment resulting from monodentate coordination or several phosphorus environments in rapid dynamic equilib-

Table 6. Observed Chemical Shift Values (δ, ppm vs H_3PO_4) for Solution ^{31}P NMR of Compounds $[U(ReO_4)_4(TBPO_4)]$ (**2**), $[U(ReO_4)_4(TEP_4)]$ (**3**), $[U(ReO_4)_4(T^iBP)_4]$ (**4**), $[U(ReO_4)_4(TPPO)_3(CH_3CN)]\cdot 2CH_3CN$ (**5**), $[U(ReO_4)(DPPMO_2)_3(OH)][ReO_4]_2\cdot 2CH_3CN$ (**6**), and the Free Ligand in Deuterated Solvent at 298 K

compd	ligand system	solvent	free ligand	U(IV) perrhenato compound
5	TPPO	MeOD	32.49	46.67
2	TBPO	CD_3CN	48.97	74.78
6	$DPPMO_2$	pyridine	23.67	39.79, 26.86, 22.54, 21.42
3	TEP	MeOD	−1.14	−3.97
4	T^iBP	MeOD	−1.08	−5.33

rium. However, for the bidentate $DPPMO_2$ ligand, four peaks are observed which indicates a number of different phosphorus environments and/or inequivalence of the P═O donor ligands. All the spectra are provided as Supporting Information, and the ^{31}P NMR peak positions for all complexes and free ligands at 298 K are presented in Table 6.

A broad signal is observed at 298 K for $[U(ReO_4)_4(TPPO)_3(CH_3CN)]\cdot 2CH_3CN$ (**5**) in MeOD. As the temperature is lowered to 228 K, a sharper peak is resolved at 46.67 ppm, a shift of approximately 0.75 ppm upfield, which implies several TPPO chemical environments in rapid exchange at room temperature. As the temperature is lowered, a shoulder on the main peak emerges at 47 ppm indicating an exchange process is still occurring at 228 K. These spectra confirm that TPPO remains coordinated with a peak for free ligand at ca. 32 ppm not observed at any temperature. This observation is consistent with the solution IR data. The different chemical environments for coordinated TPPO are observed at very similar chemical shift values, perhaps indicative of changes in structure in one complex, perhaps between two different coordination environments. Similar molecular motion processes have previously been observed for both U^{IV} and Th^{IV} compounds through variable-temperature ^1H NMR.[36]

Dissolution of $[U(ReO_4)_4(TBPO)_4]$ (**2**) in CD_3CN gives a broad peak at room temperature at 74.5 ppm which sharpens upon cooling and is accompanied by the emergence of an additional peak at approximately 73 ppm that increases in intensity as the temperature is lowered further. No peaks are observed at ca. 49 ppm relating to free ligand, again consistent with the solution IR data. This clearly shows two phosphorus environments, which are in rapid exchange at room temperature. At lower temperatures this exchange process slows, enabling two separate peaks to be observed for each chemical environment. This may result from different species in solution with a different number of coordinated TBPO ligands and possibly a different number of coordinated solvent molecules. However, it may also be due to fluxional processes in one complex as previously indicated for the ^{31}P NMR spectrum of **5**.

The spectrum for $[U(ReO_4)(DPPMO_2)_3(OH)][ReO_4]_2$ (**6**) is very difficult to interpret. At room temperature, the two major peaks at 26.86 and 21.42 ppm occur at values very close to the value for uncoordinated $DPPMO_2$ (23.67 ppm) in pyridine. However, for $[UO_2(ReO_4)(DPPMO_2)_2]$ and $[UO_2(TcO_4)(DPPMO_2)_2]$,[3] peaks at 42.1 and 40.7 ppm, respectively, in CD_3CN are observed for the two complexes, ca. 20 ppm more positive that uncoordinated $DPPMO_2$ in the same solvent. The peak at 21.42 ppm and a smaller peak at 22.54 ppm coalesce and broaden as the temperature is lowered, with the peak at 26.86 ppm also broadening to some extent. As it is not feasible to relate all three bands to uncoordinated $DPPMO_2$, then at least two must be related to U(IV)-coordinated $DPPMO_2$ with the unexpected peak positions perhaps related to paramagnetic shifting from the U^{IV} center (although this does not appear to broaden the bands greatly or affect the spectra for **2**−**5**). The low intensity peaks broadening and sharpening as a function of temperature between ca. 39 and 45 ppm are more indicative of coordinated $DPPMO_2$.

For the T^iBP complex (**4**), as the temperature is lowered, the single phosphorus peak is broadened and reduced in intensity. This is suggestive of a rapid ligand exchange process at room temperature slowing in the NMR time scale as the temperature is lowered. From the comparison with the results of infrared spectroscopy, it is postulated that the exchange process is between coordinated and uncoordinated T^iBP although it has not been possible to separate out two distinct peaks. For the TEP complex (**3**), the variable-temperature ^{31}P NMR spectra obtained are almost identical to those observed for $[U(ReO_4)_4(T^iBP)_4]$ (**4**), and a similar chemical process is also believed to occur.

Conclusion

Three isostructural U^{IV} complexes with coordinated perrhenate, general formula $[U(ReO_4)_4(L)_4]$ (where L = TBPO (**2**), TEP (**3**), or T^iBP (**4**)), have been synthesized through the photoreduction of ethanolic $\{UO_2\}^{2+}$ solutions containing the appropriate additional ligands. These complexes have also been synthesized through a more direct route using the new starting material $U(ReO_4)_4\cdot 5H_2O$ (**1**), as have two additional compounds, $[U(ReO_4)_4(TPPO)_3(CH_3CN)]\cdot 2CH_3CN$ (**5**) and $[U(ReO_4)(DPPMO_2)_3(OH)][ReO_4]_2(MeCN)_2$ (**6**). All six compounds have been spectroscopically characterized, with **2**, **3**, **5**, and **6** also crystallographically characterized. A crystallographic study of **4** has confirmed connectivity, but full refinement was not possible in this case. Compounds **2**−**6** exhibit eight-coordinate geometry with up to four perrhenate groups in addition to three ($DPPMO_2$ and TPPO) or four (TEP, T^iBP, TBPO) coordinated organic ligands. Eight-coordinate geometry is achieved through coordination of a solvent molecule to the U^{IV} metal center in the case of **5** and OH^- in the case of **6**.

A solid-state infrared spectroscopic study of all six compounds has been carried out, and this supports the crystallographic data with vibrations assigned to coordinated organic P═O donor ligands and monodentate perrhenate groups, with potential chelate coordination of $[ReO_4]^-$ in **1**. Additional solution spectroscopic studies (infrared and ^{31}P NMR) have given evidence that U^{IV} has a preference to

(36) (a) Folcher, G.; Kiener, C.; Rigny, P.; Virlet, J. *Chem. Phys. Lett.* **1978**, *60*, 135. (b) Domingos, Â.; Marcalo, J.; Pires De Matos, A. *Polyhedron* **1992**, *11*, 909.

coordinate to phosphine oxide ligands rather than perrhenate and for perrhenate over phosphate ligands in the presence of coordinating solvent, as is also clearly shown in a structural comparison of **2** and **3**. This may have implications for solvent extraction processes in the nuclear industry, which are often undertaken with tri-*n*-butyl phosphate. It could be postulated that the mechanism of U^{IV} oxidation to $\{UO_2\}^{2+}$ by $[TcO_4]^-$ includes the initial formation of an inner sphere complex.

Acknowledgment. We thank EPSRC and the Research and Technology group at BNFL (now Nexia Solutions) for funding.

Supporting Information Available: Crystallographic data in CIF format, TGA data, and both IR and ^{31}P NMR spectroscopic data. This material is available free of charge via the Internet at http://pubs.acs.org.

IC0507971